# Wind Turbine Fault Detection and Identification Through PCA-Based Optimal Variable Selection

Yifei Wang, Xiandong Ma, and Peng Qian

***Abstract*—An effective condition monitoring system of wind turbines generally requires installation of a high number of sensors and use of a high sampling frequency in particular for monitoring of the electrical components within a turbine, resulting in a large amount of data. This can become a burden for condition monitoring and fault detection systems. This paper aims to develop algorithms that will allow a reduced dataset to be used in wind turbine fault detection. This paper first proposes a variable selection algorithm based on principal component analysis with multiple selection criteria in order to select a set of variables to target fault signals while still preserving the variation of data in the original dataset. With the selected variables, this paper then describes fault detection and identification algorithms, which can identify faults, determine the corresponding time and location where the fault occurs, and estimate its severity. The proposed algorithms are evaluated with simulation data from PSCAD/EMTDC, Supervisory control and data acquisition data from an operational wind farm, and experimental data from a wind turbine test rig. Results show that the proposed methods can select a reduced set of variables with minimal information lost whilst detecting faults efficiently and effectively.**

***Index Terms*—Variable selection, principal component analysis, fault detection, condition monitoring, wind turbines.**

## I. Introduction

THE importance of continuous and autonomous condition monitoring (CM) and fault detection systems for engineering applications has increased dramatically in the past decades. This is particularly the case for wind power, as turbines are often deployed in remote and harsh environments. CM techniques can help improve the performance and reliability of the wind turbines (WTs) [1]. According to IRENA, the operation and maintenance cost of a WT is between 10%–25% of the total cost of electricity [2], [3]. With increasing size and complexity of turbines, and the move to building more offshore wind farms, maintaining the performance and reliability of WTs technically and financially has become a challenge.

Based on the information collected from sensors, a CM system monitors and identifies potential anomalies and predicts WT's future operation trend, allowing preventative maintenance of the turbine to be undertaken. With a sufficiently early warning, it is possible to reduce down-time and avoid component damage due to unexpected failures. Moreover, by continuous monitoring of the WT's components, the life cycle of turbine components can be estimated, and maintenance activities scheduled accordingly to optimize asset management.

An effective CM system for wind turbines relies upon algorithms designed for accurate fault detection and prediction; however, there are two major issues. The first of these is associated with the amount of data generated by sensors. Typically, a wind turbine CM system monitors approximately 150–250 variables [4], and its sampling rate depends on the nature of the monitoring system, ranging from 0.002 Hz (e.g., SCADA) to $>$10 kHz data for dedicated diagnostic purposes. The need to store and process these data increases the cost, and complicates the performance of both the CM system and the interpretation of its output. The second issue relates specifically to sensor reliability. Elouedi *et al*. and Guo *et al.* have both pointed out issues regarding the accuracy and accountability of sensors used for pattern recognition and fault identification and diagnosis [5], [6]. For a CM system, the accuracy of data acquired from sensors has a pronounced impact on performance. Moreover, the use of a large number of sensors, and hence monitoring variables, may reduce the overall reliability of the sensor system.

Research into optimal sensor selection has been carried out for many different applications. An entropy-based selection technique for condition monitoring for aerospace propulsion was proposed in [7]. Sensor selection for target tracking to manage sensor network topology, such as reduction of energy use and prolonging network lifetime, can be found in [8]. In addition, filtering and estimation methods for nonlinear tracking problems, using Cramer-Rao bound criteria-based sensor selection, was presented in [9]. It has been proven that there are fewer outputs from the filter/estimator than direct input measurements. However, the methods referenced above require the usage of all data for prediction and for providing improved estimated outputs. Hovland *et al*. suggested a stochastic dynamic programming method to solve the sensor selection problem for robotic systems in real time [10]. Moreover, an experimental design approach was proposed by Kincaid *et al.* to find effective locations to control and sense vibration for a complex truss structure built at the NASA Research Center through a discrete D-optimal design method [11]. This method aims to find a set of observation points that have the maximum determinant of the Fisher Information matrix. Considering WT condition monitoring,

Manuscript received March 5, 2017; revised August 11, 2017 and December 5, 2017; accepted January 29, 2018. Date of publication February 6, 2018; date of current version September 18, 2018. This work was jointly supported by the UK Engineering and Physical Sciences Research Council under Grant EP/I037326 and the Engineering Department at Lancaster University. Paper no. TSTE-00148-2017. *(Corresponding author: Xiandong Ma.)*

The authors are with the Department of Engineering, Lancaster University, Lancaster LA1 4YW, U.K. (e-mail: y.wang42@lancaster.ac.uk; xiandong.ma@lancaster.ac.uk; p.qian@lancaster.ac.uk).

Color versions of one or more of the figures in this paper are available online at http://ieeexplore.ieee.org.

Digital Object Identifier 10.1109/TSTE.2018.2801625

Zhang *et al.* implemented a parallel factor analysis of SCADA data, preserving relevant information for feature extraction and hence allowing the identification of different operation conditions of a WT through K-means clustering [12]. The authors of this paper have also carried out a study of PCA-based variable selection for a WT through maximizing data variability [13].

In this paper, a multivariate PCA-based variable selection algorithm is proposed for targeting fault signals of wind turbines. The proposed algorithm introduces a cost function with multiple criteria, such that the selected variables not only maximize dataset variability, but also contribute the most to a specific fault signal. Moreover, it has the potential of reducing the number of sensors installed through estimation of the least significant variables. Two fault diagnosis techniques are then proposed using the variables obtained from the selection algorithm. The first method detects anomalies based on the Hotelling $T^2$ statistic, making use of its identification capability by decomposing this statistic through an instantaneous energy calculation. The second method estimates fault severity by establishing an empirical model related to a specific fault using principal component (PC) coefficients. In both cases, only limited prior knowledge of the system is required, as the input dataset is obtained from the proposed selection algorithm.

The remainder of this paper is organized as follows. A general overview of PCA is first given in Section II, followed by a description of the targeted variable selection algorithm and the anomaly detection algorithms. In Section III, the data used in the evaluation process are described, including simulation data, SCADA data, and experimental data. These data are used to demonstrate the robustness of the proposed methods in Section IV. Results are also presented in this section. Finally, conclusions and ideas for future research are discussed in Section V.

## II. PCA Based Detection and Identification

PCA has been widely used in dimension reduction and feature extraction [14], [15]. By maximizing the variance in data, it captures the dominant features in an N-dimensional dataset in descending order through an orthogonal transformation. Thus the transformed data are linearly independent and are referred to as the principal components (PCs). The PCs are commonly obtained through Single Value Decomposition (SVD) of the covariance matrix $\boldsymbol{S}$ ($\boldsymbol{S} = \boldsymbol{X}\boldsymbol{X}^{\mathbf{T}}$) of the original dataset $\boldsymbol{X}$. For a dataset $\boldsymbol{X}$ with dimension of $(n \times p)$, where $p$ is number of variables and $n$ is number of samples, the transformed PCs, $\boldsymbol{Z}$, are calculated from the covariance matrix $\boldsymbol{S}$ where it satisfies,

$$\boldsymbol{U'SU} = \boldsymbol{L} \tag{1}$$

where $\boldsymbol{L}\,(l_1, l_2, \ldots, l_p)$ are the eigenvalues of $\boldsymbol{S}$, which can be solved from the characteristic equation $|\boldsymbol{S} - l\boldsymbol{I}| = 0$. The eigenvalues $l_1, l_2, \ldots, l_p$ are also the variances of each PC and the sum of $\boldsymbol{L}$ equals the sum of the variance of the original variables.

After obtaining these eigenvalues, the corresponding eigenvectors $\boldsymbol{U} = \{u_i\}$, where $u_i$ is column of $\boldsymbol{U}, u_i = (u_{1i}, u_{2i}, \ldots, u_{pi}), i = 1, \ldots, p$, can be calculated. The eigenvector $\boldsymbol{U}$ is referred to as the loadings, representing the correlations between the variables and PCs. The relationship between the PCs, $\boldsymbol{Z}\,(z_1, z_2, \ldots, \mathrm{z}_p)$, and the original dataset $\boldsymbol{X}\ (n \times p)$ is expressed as $\boldsymbol{Z} = \boldsymbol{U}X$. It has been proven that, by retaining $q\,(q < p)$ PCs, the dimensionality of the data can be reduced significantly, with only minor data variability being sacrificed [16].

### A. Targeted Variable Selection

Optimal variable selection techniques for statistical applications have been proposed by Jolliffe and Beale *et al*. [17]–[19]. The idea was to establish a relationship between the transformed PCs and the original variables, hence achieving dimension reduction with minimal loss in information compared to the original dataset. Previous studies by the authors of this paper [13] adopted similar approaches to carry out variable selection for wind turbine condition monitoring based on data variability. It has been demonstrated that the technique can reduce the dimensionality of the dataset while still maintaining maximum information.

In this paper, a selection method that targets a specific fault signal is proposed, namely the T selection method. The proposed algorithm not only maximizes variance and maintains the uncorrelatedness among the selected variables but also seeks to preserve the underlying features regarding the fault signal/variable within the retained dataset. The selection algorithm can be divided into two steps. First, the PCs are selected based on the equation below,

$$\mathcal{R}_{\boldsymbol{j}}^{\boldsymbol{pc}} = \arg\min_{i \in p} \left(r_{i,j}^2 - r_{tar,j}^2\right),\ j \in q \tag{2}$$

where $\mathcal{R}^{\boldsymbol{pc}}$ refers to the set of $q$ PCs to be selected by minimizing the difference of the squared correlation coefficient between $r_{i,j}^2$ and $r_{tar,j}^2$, and $r_{i,j}^2$ is the squared correlation coefficient between the $i$th variable and $j$th PC and $r_{tar,j}^2$ is the squared correlation coefficient between the targeted variable and the $j$th PC. The squared correlation is calculated by,

$$r_{i,j}^2 = \left\{ \frac{\sum_{i=1}^{p} (x_i - \bar{x}_i)(z_j - \bar{z}_j)}{\sqrt{\sum_{i=1}^{p} (x_i - \bar{x}_i)^2 \sum_{j=1}^{p} (z_j - \bar{z}_j)^2}} \right\}^2 \tag{3}$$

where $\bar{x}_i$ and $\bar{z}_j$ are the mean value of $x_i$ and $z_j$, respectively. The equation is also equivalent to,

$$r_{i,j}^2 = l_i u_{i,j}^2 \tag{4}$$

where $l_i$ and $u_{i,j}$ are the corresponding eigenvalue and loadings obtained from the SVD.

In the second step, the corresponding original variables are identified from the retained PCs, based on (5),

$$\mathcal{R}_{\boldsymbol{j}}^{\boldsymbol{var}} = \arg\max\ \boldsymbol{u}_k,\ j \in q,\ k \in \mathcal{R}^{pc} \tag{5}$$

$\mathcal{R}_{\boldsymbol{j}}^{\boldsymbol{var}}$ is updated at every iteration and the stopping criteria for the iterations is set to the number of variables to be retained, found by using a SCREE plot. This plot visually assesses which PC components explain most of the variability in the data using cross validation techniques [16], [17].

Once a set of variables is retained, three performance measures are used in order to evaluate the selection algorithm. The

three measures are the cumulative percentage partial variance (*cppv*), the average correlation coefficient ($\bar{r}$) and the percentage information entropy ($\eta_e$). Each of these measures analyzes a different aspect of the retained dataset [13].

### *B. Hoteling's $T^2$ Method*

The Hoteling's $T^2$ statistic is often used in process control and monitoring [20], [21]. In addition, the $T^2$ statistic has been applied to detect faults in wind turbine gearboxes and pitch motors [22], [23]. In ref. [23], fault identification was performed by relying on the relative contribution index of the original measurement to the overall $T^2$ statistic through decomposition. However, the variables used in ref. [23] are based on prior knowledge of the measurements and the investigation of alarm logs. In this paper, two improvements are made for the Hotelling's $T^2$ method. Firstly, the dataset used for anomaly detection and identification is obtained from the T selection algorithm, as described in the preceding subsection. Secondly, a PC energy-based method is used to decompose the $T^2$ statistic to perform fault identification.

As can be shown, the original dataset $\boldsymbol{X}$ is estimated using the first $q$ PCs,

$$\boldsymbol{X} = \boldsymbol{Z}_q \boldsymbol{U}_q^T + \boldsymbol{E} \tag{6}$$

where $\boldsymbol{E}$ is the residual matrix signifying the amount of information not explained by the PCA model. In the perspective of statistical monitoring, Hotelling's $T^2$ is commonly found by,

$$\boldsymbol{T}^2 = \boldsymbol{X}^T \boldsymbol{U}_q \boldsymbol{L}_q^{-1} \boldsymbol{U}_q^T \boldsymbol{X} = \boldsymbol{Z}_q^T \boldsymbol{L}_q^{-1} \boldsymbol{Z}_q \tag{7}$$

where $\boldsymbol{U}_q$ and $\boldsymbol{L}_q$ are the eigenvectors and eigenvalues of the first $q$ PCs, respectively. The $T^2$ statistic is monitored continuously, and the process is considered abnormal if the statistic is above a threshold as defined below,

$$T_\alpha^2 = \frac{q\,(n\ -\ 1)}{n\ -\ q} F_{q,n-q,\alpha} \tag{8}$$

where $F_{q,n-q,\alpha}$ is the critical point of the $F$ distribution with $n$ and $n-q$ degree of freedom. The significance level $\alpha$ varies depending on the data, and is typically between 90% and 95%.

For the period where anomalies have been identified, the relative contribution of $i$th PC, i.e., the $TC_i$, to the $T^2$ statistic can be decomposed by calculating the instantaneous energy,

$$TC_i = (|z_i|)^2 \tag{9}$$

where $z_i$ is the $i$th unscaled PC.

Fig. 1 shows the process of anomaly detection and identification. During the training stage, a dataset from a healthy turbine, that has a mean value of $\bar{x}$, is normalized to zero mean and unit variance. Variables are selected via the above T selection algorithm for a predefined fault signal. Then the PCA model is created; its $T^2$ statistic and threshold value $T_\alpha^2$ are calculated using (7) and (8) respectively. During the testing stage, the data are normalized using the data from the healthy turbine. The PCA model and the $T^2$ statistics are also calculated for the turbine data being evaluated. If any of the $T^2$ statistics exceed the threshold value $T_\alpha^2$, as calculated from the normal operational

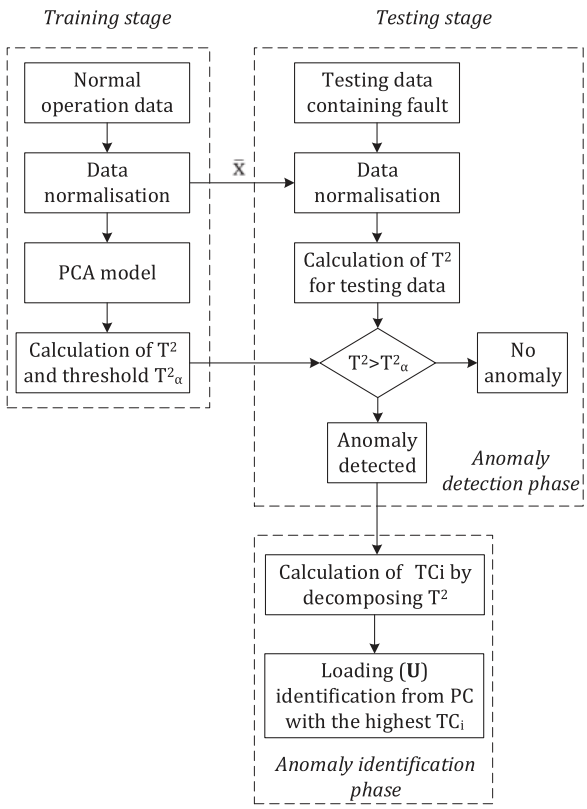


Fig. 1. Block diagram of the Hotelling's $T^2$ based fault detection and identification algorithm.

data, the measurement is considered to be an anomaly. For the period where anomalies are present, the $T^2$ statistics are decomposed using (9) to determine which variables have the highest contribution to the anomalies.

### *C. Feature Based Fault Severity Estimation*

In this section, an empirical model is proposed to detect a specific fault, and then to estimate its severity under various operation conditions. This is achieved using retained variables from the T selection algorithm. Suppose there is a set of variables $\boldsymbol{X}$ with dimension $(n \times q)$ obtained from the T selection algorithm and related to a specific type of fault. To build the detection model, measurement data for these variables are collected multiple times $\boldsymbol{X}^d$ at different fault severities, where $d$ indicates the index for each severity. PCA is carried out for all these datasets, where $d$ eigenvector matrices $\boldsymbol{U}\,(q \times q)$ and $d$ eigenvalue vectors $\boldsymbol{L}\,(q \times 1)$ are obtained. It can be shown that there is a relationship between the fault severity $S_v$ and eigenvalues $\boldsymbol{L}$ and eigenvectors $\boldsymbol{U}$, described as,

$$S_v = f\,(u_{i,j}, L_j)\,,\ \ 1 < i < q,\ 1 < j < q \tag{10}$$

The relationship function $f$ is fault dependent, by which the fault can be identified even at an incipient stage.

## III. Case Study - Monitoring Data

### A. Wind Turbine Simulation Data

A 2 MW doubly-fed induction generator (DFIG) wind turbine model with grid connection is simulated in PSCAD/EMTDC. The simulation is based on the benchmark model developed by PSCAD [24]. The model comprises a mechanical model of a turbine, which simulates the blades' aerodynamic behavior, a mechanical shaft, a generator, an AC-DC-AC converter, and a grid network. This simulation is primarily used for investigating the performance of wind turbine's transient and steady state conditions. The behavior of the turbine during normal and faulty operations can also be analyzed. Simulations are performed using wind speed data collected at the Hazelrigg site near Lancaster University, where a 2.1 MW wind turbine is installed and operating. Measurements are taken from both internal and external nodes of the simulated system under different operational conditions. Computer simulations of a wind turbine incorporating a permanent magnetic synchronous generator (PMSG) with a grid connection have also been created. It is worth mentioning that, in this paper, simulation data are used for severity estimation of the faults in the turbine using the proposed feature-based fault detection method.

### B. SCADA Data

SCADA data contains a large amount of information regarding the operational and performance status of WTs. Although SCADA data generally have low sampling rates, they can provide an overview of a turbine's operational and performance status and condition, and have been employed widely by researchers as the basis for CM systems. The SCADA data used in this paper are taken from an operational wind farm with 24 turbines in total. The condition of each turbine is described by 128 variables, including temperatures, vibrations, electrical parameters, wind speed, and digital control signals. The data are sampled at an interval of one second, but are averaged over 10 minutes and then stored on a database for 15 months. Preprocessing of the data is performed to eliminate digital signals, constant readings, and error signals due to faulty sensors, which are ineffective to the PCA analysis. Fault-free data are needed to train the model with the proposed detection and identification algorithm. For SCADA data, the active power versus wind speed curve, i.e., the S-curve, can be adopted to identify if the data are fault-free, as concluded by S. Gill *et al.* [25]. The turbine that yields an ideal S-curve after pre-processing is selected as the reference healthy turbine.

### C. Experimental Wind Turbine Test Rig

Experimental data from a WT test rig have also been collected and used for further evaluation of the proposed algorithm. The rig allows specific faults, such as phase-to-phase short circuit faults, to be applied. The physical layout and overall schematic of the test rig is shown in Fig. 2 and Fig. 3, respectively. The rotation of the turbine and the aerodynamics of the blade are simulated by a computer and emulated with an ABB 11 kW squirrel-cage induction motor controlled by a frequency drive.

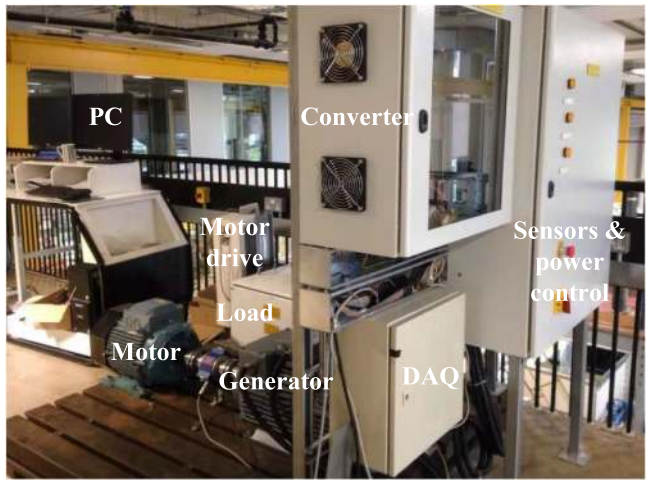


Fig. 2. Layout of the wind turbine test rig developed at Lancaster University.

The induction motor is directly coupled to a 3 kW PMSG generator from Mecc Alte. The use of this induction motor incorporating the variable frequency drive can ensure it provides the required torque to operate the generator at different speeds. The AC-DC-AC converter consists of an uncontrollable AC-DC rectifier, a DC-link capacitor and a DC-AC inverter. The rectifier converts the mains voltage to a DC voltage of 540 V for DC-filtering and energy buffering via the DC-Link capacitor. The IGBT inverter then converts the DC power into an AC power at the desired output voltage and frequency via the filter ($L_f$ and $C_f$ in Fig. 3). A DC-link capacitor discharging circuit ($R$ and $S_d$) is also added to discharge the capacitor after the tests. The test rig operates in an island mode, where all the generated power from the AC-DC-AC converter is dissipated to an off-the-shelf resistive load bank via a variable transformer. A number of transducers and sensors are installed in the test rig to collect data for control and monitoring purposes, including AC currents and voltages before and after the converter, and the DC-link current and voltage. All signals are interfaced to a data acquisition card (NI USB-6229) through signal condition modules for measurement data logging. The test rig is controlled by a computer running LabVIEW, allowing real time operation and measurements.

Peripheral components such as circuit breakers (CB) and switches are also used in the test rig to assist the components operation and for safety purposes. Due to safety issues, short circuit faults are simulated under a controlled environment where a resistance is added between phases to limit the current. A switch is used to activate the fault for a given time duration during operation of the test rig. Experiments are also performed at a low-voltage level with constant wind speeds.

## IV. Results and Analysis

### A. Targeted Variable Selection

*1) SCADA Data:* Considering initially the SCADA data, two types of fault have been studied: a gearbox fault and a generator-related fault. These faults were found by examining the SCADA

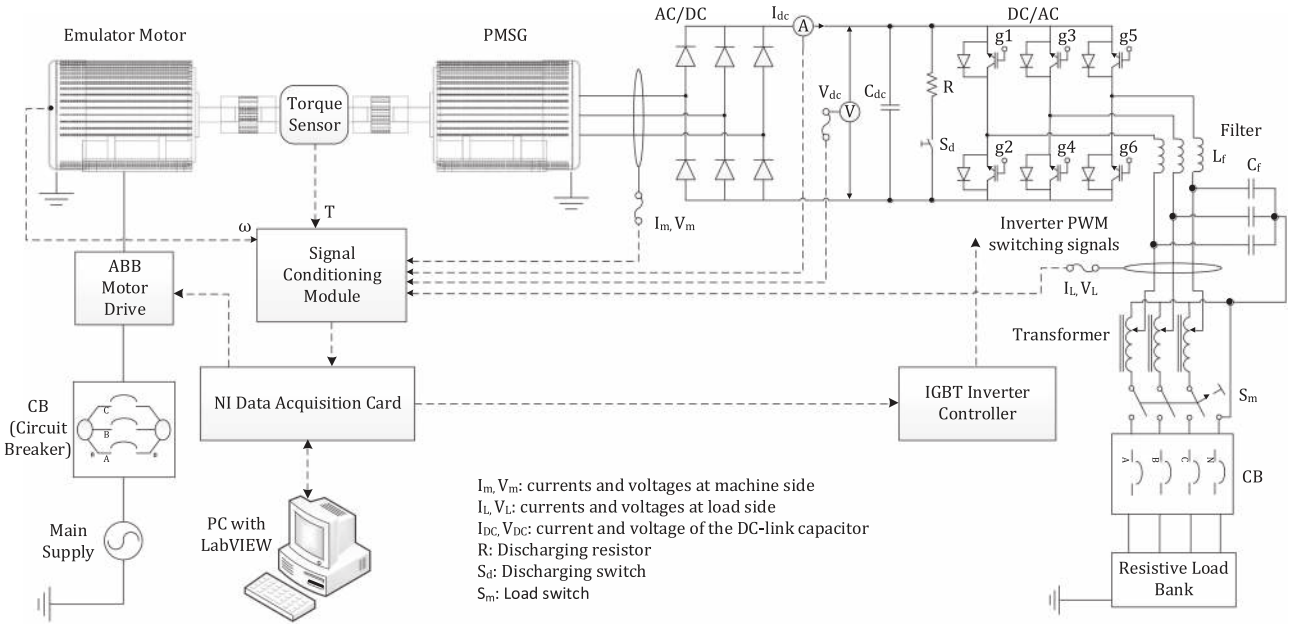


Fig. 3. Schematic block diagram of the wind turbine test rig.

TABLE I
PERFORMANCE MEASURES OF T SELECTION ALGORITHM WITH SCADA DATA

| Type of data | Original data | Gearbox fault | Generator fault |
|---|---|---|---|
| Target signal | | Gearbox bearing temperature | Generator winding temperature |
| Cumulative variance, *cppv* | 100% | 97.11% | 97.42% |
| Average correlation, $\bar{r}$ | 0.3412 | 0.0677 | 0.0588 |
| Percentage entropy, $\eta_e$ | 100% | 75.91% | 78.09% |

data together with the alarm log. A total of 77 variables were obtained after pre-processing, consisting of electrical variables, mechanical variables (angular speeds and vibrations), and temperatures. Of these, 35 variables were chosen to be the threshold for the selection algorithm, based on SCREE plot analysis. The target variables, and the respective performance measures for both fault-free data and data from the faulty turbines are given in Table I.

It can be seen that both datasets have a *cppv* above 97%, indicating the retained variables accommodate a high percentage of the variance seen in the original dataset. Moreover, there are significant reductions in the average correlation for both datasets (0.0677 and 0.0588), compared to the original data (0.3412). This implies a very low redundancy amongst the retained variables. Finally, reasonable percentage entropies are also obtained, with approximately 75.91% and 78.09% of the baseline value respectively.

In general, parameters such as wind speed, pitch angle, environmental conditions (e.g., pressure, wind direction), and vibrations are selected. It should be noted that the variables selected by the T selection algorithm should share common features with the targeting variable in the reduced dimensional space; but this does not necessary mean the selected variables must be physically close to it. For example, for a gearbox fault, the gearbox bearing temperature is used as the targeting variable; this does not mean that all variables relating to the gearbox should be retained. In fact, if that was the case, the retained variables could have very high redundancy.

*2) ANN Validation:* This section addresses the problem in which the fault feature is present in the retained variables. By adopting a NARX (nonlinear autoregressive exogenous) ANN (Artificial Neural Network) model, predictions between different input variable sets can be compared. Three different input variable sets are considered: the original dataset (without any reduction), the first $q$ PCs with a cumulative variance greater than 0.95 [16], and the retained variables from the T selection method.

The selection of input variables can greatly affect the performance of the ANN model. With regards to fault detection, it is preferable if the inputs are independent to the output variable; thus, anomalies can be identified by comparing the predicted and the actual outputs. If the input variables share common features with the fault signal (targeting variable), this could mean the model will match the actual data, even during the period of a fault. Consequently, the ANN model is used to further evaluate the retained variables from the T selection algorithm, and to demonstrate whether the fault features of interest are still present in the retained variables. A good model match is expected to be obtained, especially during the period of the fault. The ANN model established using the original dataset is used here as a benchmark, with the squared correlation coefficient, $R^2$, and the root mean squared error (RMSE) are used to quantify the model accuracy.

As an example, SCADA data with a gearbox-related fault are used for evaluation. Fig. 4 shows the actual (red) and predicted (blue) gearbox bearing temperature using different input datasets. The anomaly occurs at approximately 720 hours, where

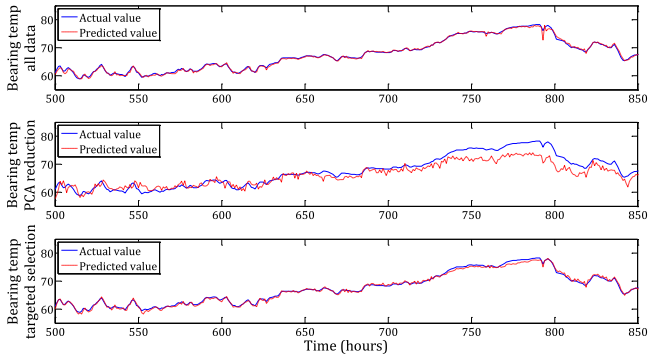


Fig. 4. Actual and predicted gearbox bearing temperatures from the ANN model for three input SCADA datasets. Top: original dataset; middle: PCA reduced dataset; bottom: dataset obtained from T selection algorithm.

the gearbox bearing temperature starts to increase to an abnormal level. It can be seen that the prediction using all of the data is very close to the actual value, with RMSE and $R^2$ of [0.276, 99.5%]. Similarly, in the case of the targeted selection data, a high model prediction is also obtained [0.397, 99.2%]. As for the PCA reduced data, it has the worst performance of [1.793, 82.3%], where there is an obvious difference between the actual and predicted gearbox bearing temperature. It is worth mentioning that, for all cases, the predictions during the fault-free period are very similar. The difference between the actual and the predicted value becomes clear when the fault begins. Based on these results, it is straightforward to conclude that the dataset retained by the T selection algorithm has captured the fault signatures from the original dataset.

### B. Hoteling's $T^2$ Method

In this section, SCADA data are used to validate the proposed Hoteling's $T^2$ detection and identification algorithm. One of the assumptions made for $T^2$ statistics is that the original data should be approximately normally distributed. Therefore, an additional pre-processing step is carried out to normalize the data by means of a Box-cox transformation.

$$x_i^{(\lambda)} = \begin{cases} \frac{x_i^{\lambda}-1}{\lambda} & \text{if } \lambda \neq 0 \\ \ln(x_i) & \text{if } \lambda = 0 \end{cases} \tag{11}$$

where $x$ is the original data and $\lambda$ is the coefficient optimized through the maximum likelihood function such that the resulting data is approximately normally distributed. The distribution of wind speed before and after this transformation is shown in Fig. 5.

*1) SCADA Data With Gearbox Fault:* The $T^2$ statistic and the threshold of the normal operating (top) and the test data with gearbox fault (bottom) are shown in Fig. 6. As can be seen in the bottom plot, between sample points 1400 to 1450 and 1510 to 1545, the $T^2$ statistic is well above the threshold. The SCADA data has a sampling rate of 10 minutes, which implies the detected anomalies lasted for a period of 8 hours. By decomposing the $T^2$ statistic, PC1 has the highest contribution index (Fig. 7, top). The loading values for PC1 are then shown

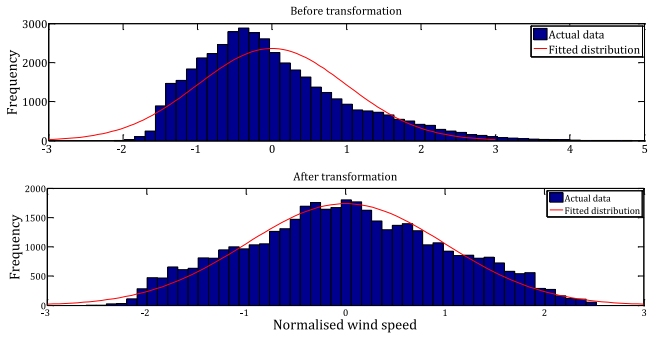


Fig. 5. Example of histogram of wind speed from SCADA data before (top) and after (bottom) the Cox-box transformation.

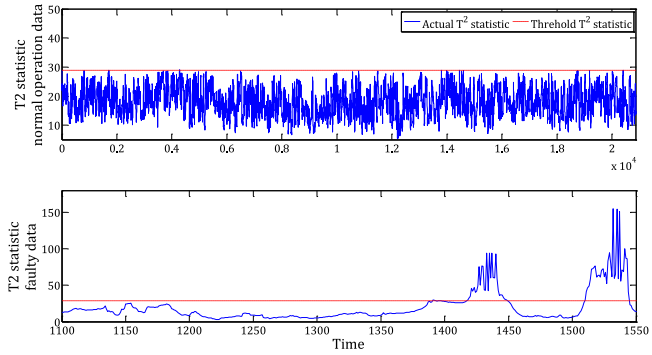


Fig. 6. $T^2$ statistic from the SCADA data with a gearbox fault. Top plot: normal operation data; bottom plot: data with a gearbox fault.

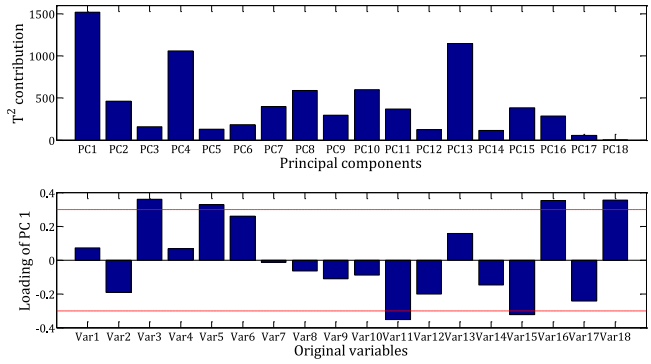


Fig. 7. Fault identification of the SCADA data with a gearbox fault. Top plot: $T^2$ contribution; bottom plot: PC loadings showing the highest contribution.

in the bottom plot of Fig. 7. Any loading, which is greater than the threshold value of 0.3, is considered significant [17].

Fig. 7 shows that the active power (*Var3*), gearbox bearing temperature (*Var18*) and gearbox oil sump temperature (*Var16*) have the top three loading values. Other variables with significant loadings are the generator bearing temperature (*Var15*), power factor (*Var5*) and pitch motor 1 RPM (*Var11*). This result indicates that the root cause of the fault might occur at the cooling system of the gearbox; hence, the gearbox bearing temperature is also increased. Furthermore, the turbine data show a reduced active power output during the faulty period, and a warning of a high gearbox temperature is also found in the alarm log. The turbine was intentionally controlled to operate at

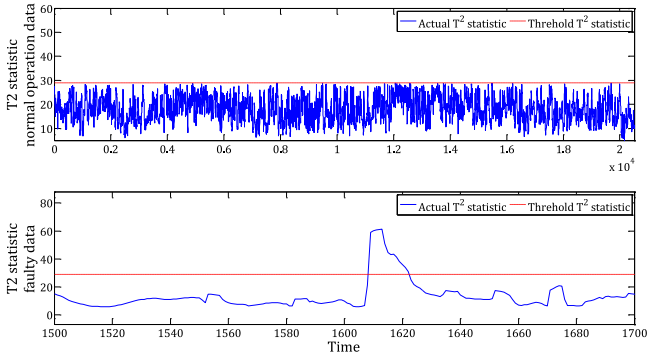


Fig. 8. $T^2$ statistic from the SCADA data with a generator fault. Top plot: normal operation data; bottom plot: data with a generator fault.

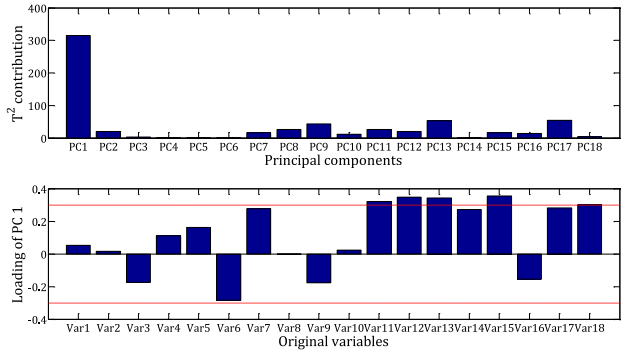


Fig. 9. Fault identification of the SCADA data with a generator fault. Top plot: $T^2$ contribution; bottom plot: loadings showing the highest contribution.

a lowered power rating in order to avoid damaging the turbine. Evidently, the anomaly is related to the gearbox.

*2) SCADA Data With Generator Fault:* Considering the SCADA data obtained from the turbine with a generator fault, the $T^2$ statistic and the corresponding decomposition are shown in Figs. 8 and 9 respectively. An anomaly is detected between sampling point 1610 and 1630, lasting for a period of 3.3 hours. It was found that the first PC is the most significant. Parameters such as the temperature of the generator cooling water (*Var13*), the generator bearing temperature (*Var15*), vibration in the z direction (*Var12*), and the temperature of the main bearing (*Var11*) have significant loading values above 0.3. The result shows that the anomaly is caused by abnormal temperature changes, which are localized in the generator. This result corresponds to findings from the analysis of data and the alarm log, where a warning of a high generator bearing temperature has been flagged. As both the main bearing and the generator bearing temperature are high, along with increased vibration, the main contributor to this anomaly is likely to be wear of the generator bearing.

Consequently, the proposed method can detect anomalies in the dataset and highlight variables contributing to it, thereby identifying and locating the fault based on the highest loading values corresponding to the most significant PC.

### C. Feature Based Fault Detection

Because the feature-based detection method requires datasets of faults at different severity levels, this section firstly considers

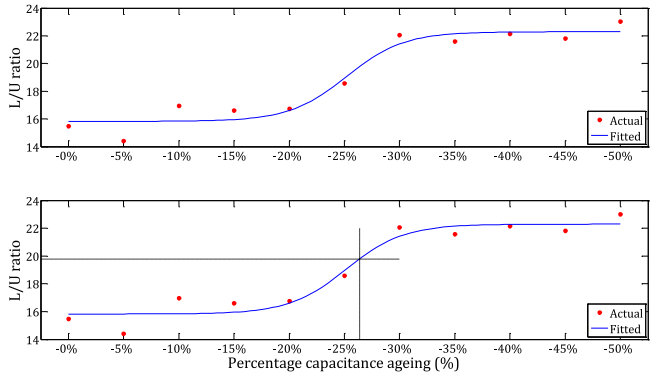


Fig. 10. Fault severity plot of simulation data with capacitor ageing fault through PCA. Top: plot of actual and fitted model of $r_{l/u}$ ratio; bottom: estimation of unknown fault severity from the established model.

simulation data with a DC-link capacitor ageing fault. The fault is simulated as a loss of capacitance at various severities, from the normal operation condition of 7800 $\mu$F at a reduction step of $-5\%$ until $-50\%$. An empirical model has been created using these data and variables obtained from the T selection algorithm. It was found that there is a clear relationship to the $r_{l/u}$ ratio between $\mathbf{L}_1^r$ (the first eigenvalue) and $\mathbf{U}_{1,1}^r$ (the first element of the first eigenvector), as shown in Fig. 10 (top). The following nonlinear function has been fitted to the data,

$$r_{l/u} = \frac{l_1^r}{u_{1,1}^r} = a\tanh\left(bS_v + c\right) + d \tag{12}$$

where tanh is the hyperbolic function; the coefficients $a$, $b$, $c$, and $d$ are estimated through nonlinear least squares by minimizing the residual, found to be 3.234, 0.9597, $-5.7903$ and 19.06, respectively. The fitted curve has a $R^2$ of 94.49%, indicating an accurate fit. It can be seen that the $r_{l/u}$ has an increasing trend when the capacitance losses increase, with the largest rise between $-15\%$ to $-35\%$.

To test the empirical model, additional data have been obtained with a different fault severity compared to those used to train the model. The $r_{l/u}$ ratio for the dataset with an unknown fault level is 19.7805. Using the inverse relationship function, as described in (13), the estimated severity $S_v$ is found to be $-26.362\%$. The actual fault level is $-27\%$, as shown in the bottom plot of Fig. 10, an error of 2.4%, implying an accurate detection and severity estimation.

$$S_v = \frac{\operatorname{arctanh}\left(\frac{r_{l/u}-d}{a}\right) - \mathrm{c}}{b} \tag{13}$$

Data obtained from the WT test rig with a phase-to-phase short circuit fault have been used to evaluate further the feature-based detection and severity estimation algorithm. Fig. 11 shows the root mean square (*rms*) value of the current (top) and voltage (bottom) under different fault severities emulated by short circuit resistance values ranging from no-fault (1 M$\Omega$), to 2000 $\Omega$, 351 $\Omega$, 135 $\Omega$, and 27 $\Omega$ respectively. Results show that, although performed with a low power rating, the experiments still reflect the transient behavior of the fault. Thus, the data have been considered to be adequate for evaluating the proposed detection method.

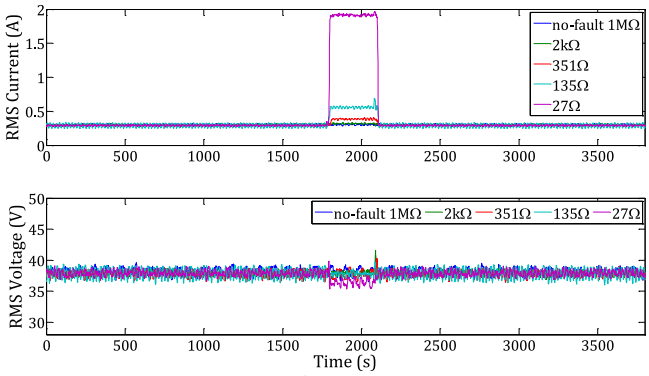


Fig. 11. Measured rms voltages and currents under the phase-to-phase fault with different fault severities.

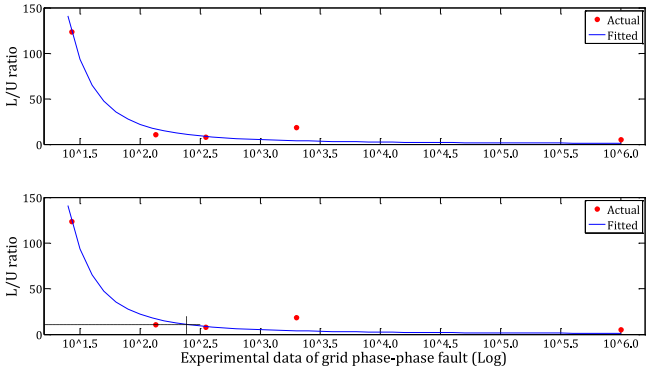


Fig. 12. Fault severity plot of the test rig data with phase-to-phase fault through PCA. Top: plot of actual and fitted model of $r_{l/u}$ ratio; bottom: estimation of unknown fault severity from the established model.

An empirical model has been obtained following the PCA of the measured line-voltages and phase-currents. The red dots in the top plot of Fig. 12 show the $r_{l/u}$ ratio of $\mathbf{L}_1^r$ and $\mathbf{U}_{2,2}^r$ (the second element of the second eigenvector) from measurements at different fault severities $S_v$. The relationship function fitted is,

$$r_{l/u} = \frac{l_1^r}{u_{2,2}^r} = a \times e^{\frac{b}{S_v}} \tag{14}$$

where the coefficients $a$ and $b$ are 0.2857 and 8.685, respectively. The fitted curve has an $R^2$ of 97.41%. It can be seen that the $r_{l/u}$ ratio increases exponentially when the fault resistance decreases, implying a more severe fault.

To test the model, additional data with an unknown fault severity is used, and the $r_{l/u}$ ratio is 10.8789. Using the inverse relationship function, as given in (15), the estimated severity $S_v$ is found to be 2.3863, as shown in the bottom of Fig. 12.

$$S_v = b \times ln\left(\frac{r_{l/u}}{a}\right)^{-1} \tag{15}$$

This corresponds to a fault resistance of 243.4 Ω with an error of only 0.2%, compared to the actual value of 243 Ω. The results show that the fault can be identified and its severity can be estimated accurately.

## V. Conclusion

In this paper, a PCA-based variable selection algorithm targeting specific fault signals is proposed for condition monitoring of wind turbines. Three performance measures (cumulative percentage variance, average correlation, and percentage entropy) have been employed to evaluate different aspects of the algorithm regarding variable selection. SCADA data exhibiting different types of fault have been used to evaluate the T selection algorithm. A dimension reduction of 45.5% is achieved for SCADA data. The retained variables also have a high *cppv* and percentage entropy, and a very low average correlation coefficient. This implies that the proposed algorithm can identify a set of variables containing sufficient information and minimum inter-correlation to diagnose the fault signals.

By adopting an ANN model, predictions between different input variable sets are compared. Results show that the model with these retained variables has a very high prediction accuracy. This has been attributed to the removal of irrelevant signals and information redundancy during the selection process, minimizing overfitting of the model.

Using the retained variables, two anomaly detection methods have been proposed: the first is capable of identifying anomalies, and the second can estimate the severity of the fault through an empirical model. Both methods have been tested with simulation data, SCADA data, and experimental data, each with different types of fault. Results have shown that the algorithms allow accurate detection, identification, and estimation of the severity of the faults. Moreover, the proposed methods require minimal human interaction once the model is built. Consequently, the method possesses great potential in developing an autonomous condition monitoring system. In future studies, the development of the algorithms in real-time for online monitoring purposes will be investigated, and selection methods based on nonlinear algorithms will be analyzed.

## Acknowledgment

The permission of use SCADA data from Wind Prospect Ltd are gratefully acknowledged.

## References

[1] F. Spinato, P. J. Tavner, G. J. W. van Bussel, and E. Koutoulakos, "Reliability of wind turbine subassemblies," *IET Renewable Power Gener.*, vol. 3, no. 4, pp. 287–401, 2009.
[2] IRENA, "Renewable energy technologies: Cost analysis series," IRENA, Abu Dhabi, UAE, Tech. Rep., Jun. 2012.
[3] Y. Lin, L. Tu, H. Liu, and W. Li, "Fault analysis of wind turbines in China," *Renew. Sustain. Energy Rev.*, vol. 553, pp. 482–490, 2016.
[4] X. Ma, "Novel early warning fault detection for wind turbine-based DG systems," in *Proc. 2nd IEEE PES Int. Conf. Exhib. Innov. Smart Grid Technol.*, Manchester, U.K., 2011.
[5] Z. Elouedi, K. Mellouli, and P. Smets, "Assessing sensor reliability for multisensor data fusion within the transferable belief model," *IEEE Trans. Syst., Man Cybern., Part B, Cybern.*, vol. 34, no. 1, pp. 782–787, Feb. 2004.
[6] H. Guo, W. Shi, and Y. Deng, "Evaluating sensor reliability in classification problems based on evidence theory," *IEEE Trans. Syst., Man Cybern., Part B, Cybern.*, vol. 36, no. 5, pp. 970–981, Oct. 2006.
[7] L. Liu, S. Wang, D. Liu, Y. Zhang, and Y. Peng, "Entropy-based sensor selection for condition monitoring and prognostics of aircraft engine," *Microelectron. Rel.*, vol. 55, pp. 2092–2096, 2015.

[8] X. Shen, S. Liu, and P. Varshney, "Sensor selection for nonlinear systems in large sensor networks," *IEEE Trans. Aerosp. Electron. Syst.*, vol. 50, no. 4, pp. 2664–2678, Oct. 2014.
[9] A. Mohammadi and A. Asif, "Consensus-based distributed dynamic sensor selection in decentralised sensor networks using the posterior Cramer-Rao lower bound," *Signal Process.*, vol. 108, pp. 558–575, 2015.
[10] G. Hovland and B. McCarragher, "Control of sensory perception in discrete event systems using stochastic dynamic programming," *J. Dyn. Syst., Meas. Control*, vol. 121, pp. 200–205, 1999.
[11] K. Kincaid and S. Padula, "D-optimal designs for sensor and actuator locations," *Comput. Oper. Res.*, vol. 29, no. 6, pp. 701–713, 2002.
[12] W. Zhang and X. Ma, "Simultaneous fault detection and sensor selection for condition monitoring of wind turbines," *Energies*, vol. 9, no. 4, 2016, Art. no. 280.
[13] Y. Wang, X. Ma, and M. J. Joyce, "Reducing sensor complexity for monitoring wind turbine performance using principal component analysis," *Renewable Energy*, vol. 97, pp. 444–456, 2016.
[14] M. D. Farrell and M. M. Russell, "On the impact of PCA dimension reduction for hyperspectral detection of difficult targets," *IEEE Geosci. Remote Sens. Lett.*, vol. 2, no. 2, pp. 192–195, Apr. 2005.
[15] A. Malhi and R. X. Gao, "PCA-based feature selection scheme for machine defect classification," *IEEE Trans. Instrum. Meas.*, vol. 53, no. 6, pp. 1517–1525, Dec. 2004.
[16] J. Jackson, *Users Guide to Principal Components*. Hoboken, NJ, USA: Wiley, 1991.
[17] I. T. Jolliffe, *Principal Component Analysis*. New York, NY, USA: Springer, 2002.
[18] E. M. L. Beale, M. G. Kendall, and D. W. Mann, "The discarding of variables in multivariate analysis," *Biometrika*, vol. 54, pp. 357–366, 1967.
[19] J. A. Cumming and D. A. Wooff, "Dimension reduction via principal variables," *Comput. Statist. Data Anal.*, vol. 52, pp. 550–565, 2007.
[20] J. MacGregor and T. Kourti, "Statistical process control of multivariate processes," *Control Eng. Pract.*, vol. 3, no. 3, pp. 403–414, 1995.
[21] D. C. Montgomery, *Introduction to Statistical Quality Control*. 7th ed. New York, NY, USA: Wiley, 2013.
[22] K. Kim, S. Sheng, and P. Fleming, "Use of SCADA data for failure detection in wind turbines," in *Proc. Energy Sustain. Conf. Fuel Cell Conf.*, Washington, DC, USA, Aug. 2011, pp. 2071–2079.
[23] H. Yang, M. Huang, and S. Yang, "Integrating auto-associative neural networks with Hotelling $T^2$ control charts for wind turbine fault detection," *Energies*, vol. 8, pp. 12100–12115, 2015.
[24] *Wind turbine application technical paper, PSCAD version 4.2, Power system simulation, CEDRAT*, Meylan Cedex, France, 2006.
[25] S. Gill, B. Stephen, and S. Galloway, "Wind turbine condition assessment through power curve copula modeling," *IEEE Trans. Sustain. Energy*, vol. 3, no. 1, pp. 94–101, Jan. 2012.

**Yifei Wang** received the B.Eng. degree in mechanical engineer from the University of Malta, Msida, Malta, in 2010, and the M.Sc. and Ph.D. degrees from Lancaster University, Lancaster, U.K., in 2011 and 2016, respectively. His research interest includes data mining, hardware and software design for condition monitoring, and fault diagnosis of the wind power generation system.

**Xiandong Ma** received the B.Eng. degree in electrical engineering in 1986, the M.Sc. degree in power systems and automation in 1989, and the Ph.D. degree in partial discharge-based high-voltage condition monitoring in 2003. He is currently a Senior Lecturer with the Department of Engineering, Lancaster University, Lancaster, U.K. His research interests include intelligent condition monitoring and fault diagnosis of distributed generation systems with wind turbines with an emphasis on analytical and experimental investigation, advanced signal processing, data mining and instrumentation, and electromagnetic NDT testing and imaging.

**Peng Qian** received the B.Eng. degree in electrical engineering and automation and the M.Sc. degree in power electronics and drives, both from Jiangsu University, Zhenjiang, China, in 2009 and 2014, respectively. Since January 2015, he has been working toward the Ph.D. degree in condition monitoring of wind turbines at Lancaster University, Lancaster, U.K. His research interests include predictive condition monitoring, data driven-based modeling, optimal energy management, and hardware-in-the-loop testing.